

# 地盤シミュレーションの高度化研究

国立研究開発法人 防災科学技術研究所  
兵庫耐震工学研究センター  
Pal Mahendra Kumar

# 目次

1. Introduction
2. Problem statement
3. Results so far
  - 3.1 Generation of analysis model
    - Eigen value analysis
    - Elastic analysis
  - 3.2 Elasto-plastic analysis
    - Parameter identification
    - Discussion of simulation result
  - 3.3 Incorporation of soil container mass in analysis model
    - Modeling of soil-container
    - Discussion of simulation results
4. Summary and future plan

# はじめに

## Damage to under-ground structures during strong earthquake



写真-1 中柱の圧壊および上床版の陥没



写真-2 妻壁(海側)のひび割れ



写真-3 電気室のひび割れ状況



写真-4 中柱の損傷

## Pictures of damage

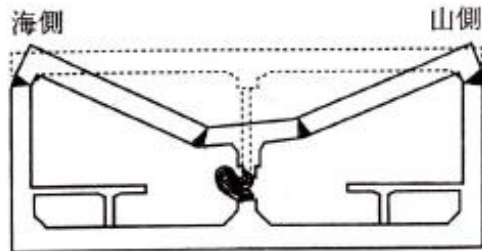


図-6 中柱(No.10)の破壊状況

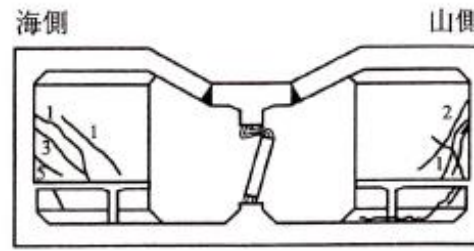


図-7 妻壁のひび割れ状況

## Schematic diagram

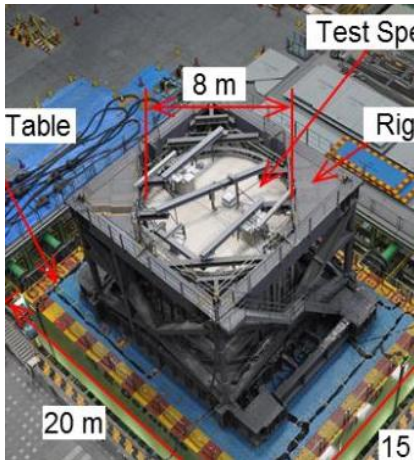
## Damage to Daikai subway station during 1995 Great Hanshin Earthquake

1. Yamato *et al*, damage to Daikai subway station of Kobe rapid transit system and estimation of its reason during 1995 Hyogoken-Nanbu earthquake ,土木学会論文集No. 537/1-35, 303-320, 1996

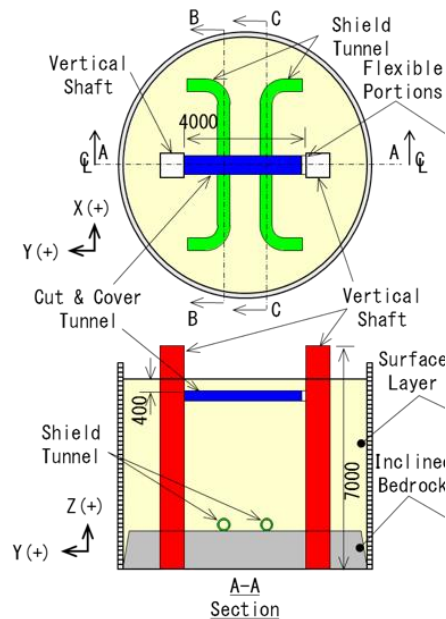
# E-Defense shake table test on soil underground specimen

- About experiment:

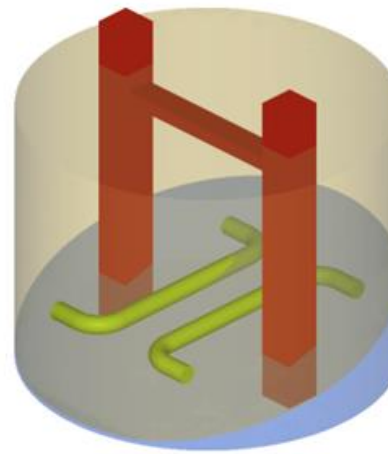
To comprehend a better understanding the soil-structure interaction a large-scale shake table test [2] was conducted at E-Defense in February 2012



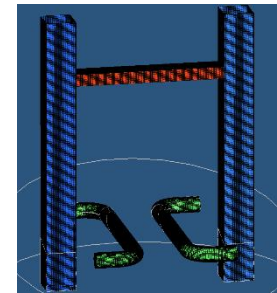
Experiment specimen



Drawing



CAD model



Analysis model

- Objectives

- Reproduction of experimental results
- Study of laminar soil container modeling

# これまでの成果

- 3.1 Generation of analysis model
- 3.2 Elasto-plastic analysis
- 3.3 Incorporation of soil container mass in analysis model

# Material properties

## Mechanical properties

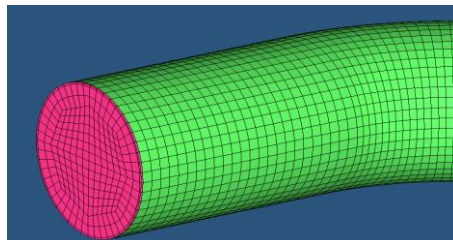
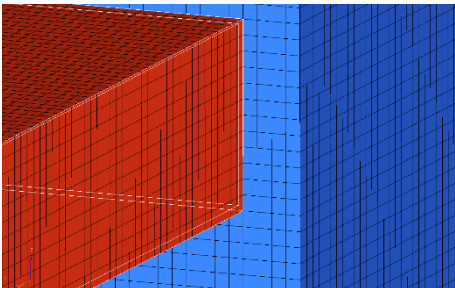
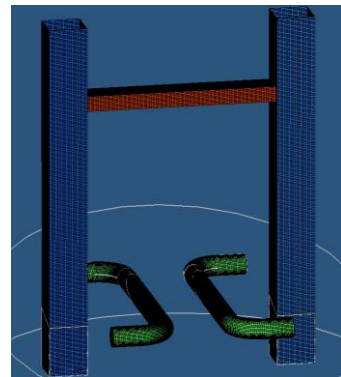
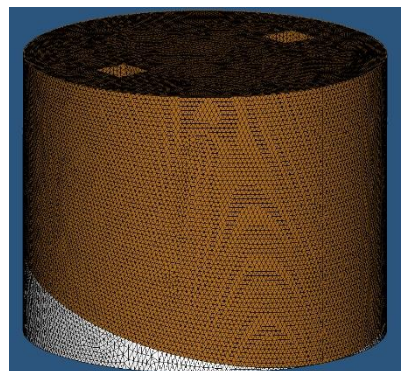
	Density (g/cm <sup>3</sup> )	Young's modulus (MPa)	Poison's ratio
Aluminum	2.70	$69.0 \times 10^3$	0.34
Acrylic Plastic	1.19	3200	0.35
Dry Sand 1	1.735	1	0.3
Dry Sand 2	1.614	12.85	
Cement mixed soil 1	2.245	$1.0 \times 10^4$	0.3
Cement mixed soil 2	2.245	88.48	0.3

## Cases considered for analysis

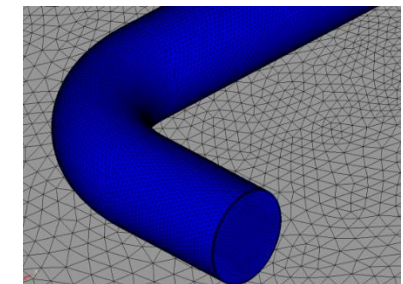
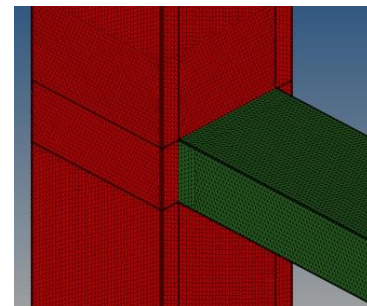
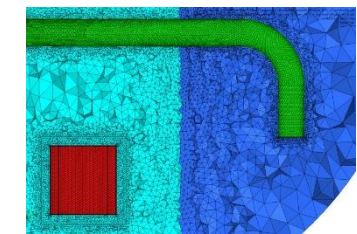
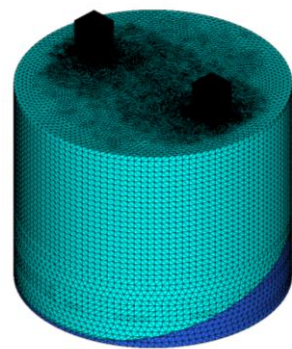
	Vertical shaft and cut-and-cover tunnel	Shield tunnel	Lower layer of soil strata	Upper layer of soil-strata	Remark
Case 1	Aluminum	Alumunium	Cement mixed soil 1	Dry Sand 1	Before experiment
Case 2	Aluminum	Acrylic Plastic	Cement mixed soil 2	Dry Sand 2	After experiment

# Analysis models

## Non-Conformity mesh model



## Conformity mesh model



**Structural component:** Hexahedral element

**Soil :** Tetrahedral element

**Interface:** using Multi-Point Constraints (MPC)

**Structural component:** Tetrahedral element

**Soil :** Tetrahedral element

**Interface:** adaptive mesh refinement

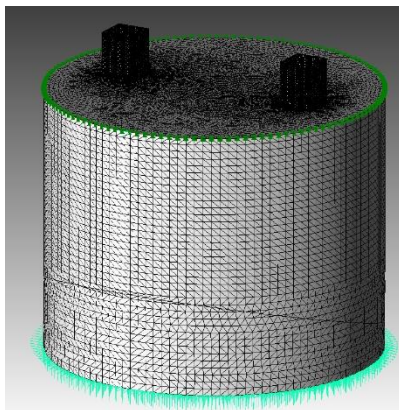
# Analysis Model

Scale of analysis

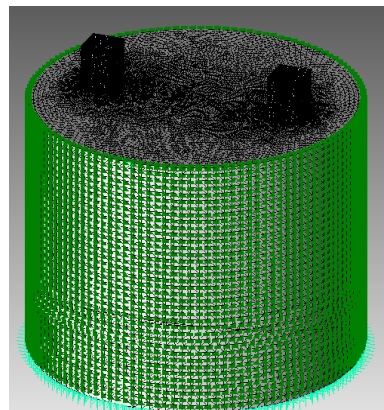
Mesh model	Elements	Nodes	Dofs
Non-conformity	1,539,094	520,959	1,562,877
Conformity	9,863,072	5,312,922	15,938,766

Computational demand\*

Mesh model	Average Computation time for each time step (min.)	Average number of CG iterations per time step
Non-conformity	64.00	13255
Conformity	1.63	1314



MPC on top model



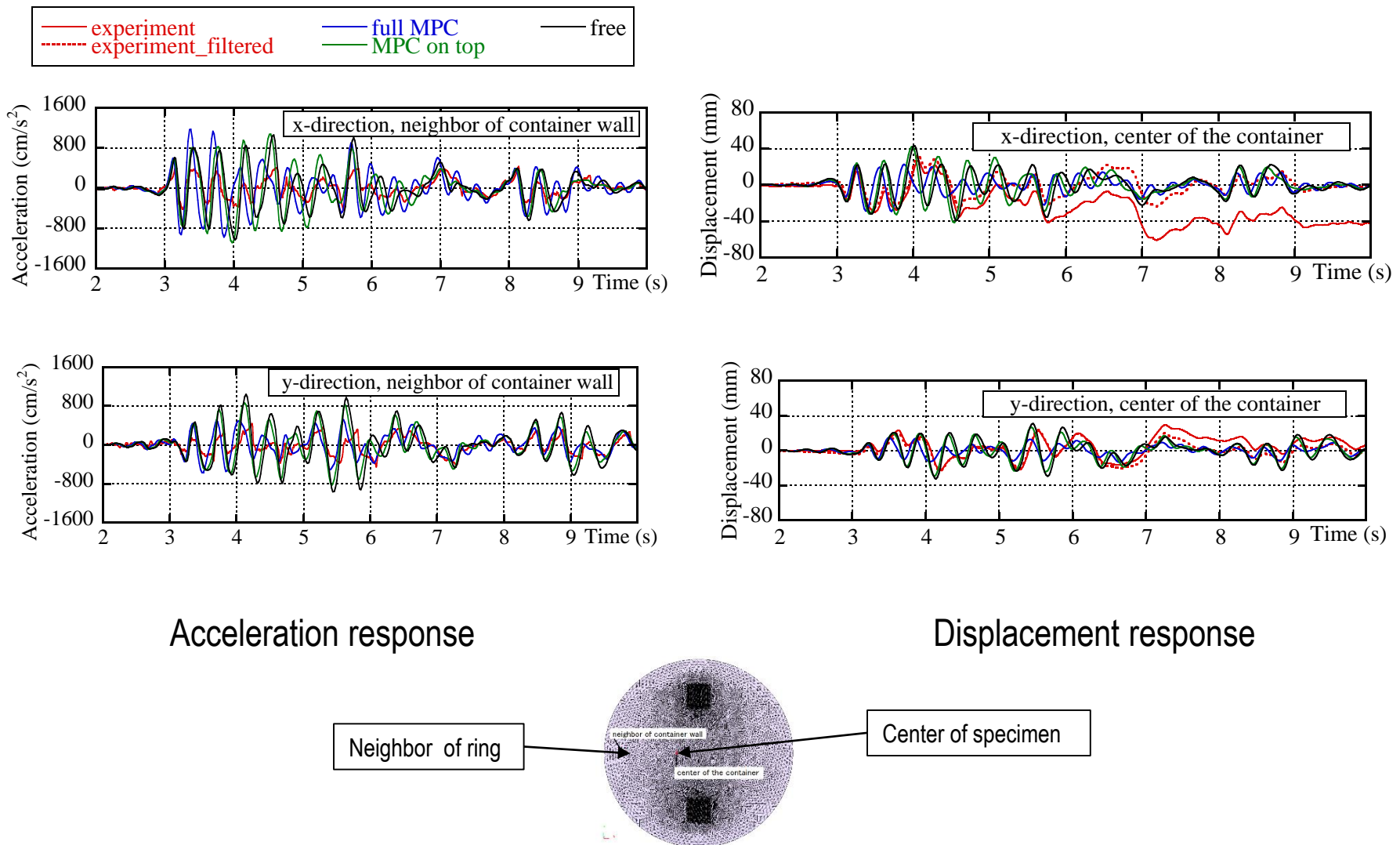
Full MPC model  
Modeling laminar soil container

Eigen value analysis

Model	1 <sup>st</sup> Mode	2 <sup>nd</sup> Mode	3 <sup>rd</sup> Mode	4 <sup>th</sup> Mode
Free	2.482	2.641	3.193	5.101
MPC on top	2.684	2.766	4.560	5.470
Full MPC	3.273	3.275	6.455	8.627
Experiment			5.27-5.56	

\*The analysis is completed on Supercomputer of NIED by using flat MPI. Analysis is performed using 128 cores of SGI Altix4700 (CPU: dual core Intel Itanium processor 1.66 GHz).

# Time history against 50% JR Takatori



MPC on top has relatively better agreement with experimental results in compare with other two models namely, Free model and Full MPC model. Therefore, MPC on Top model has been chosen as appropriate analysis model.

# Exponential Contractancy (EC) model

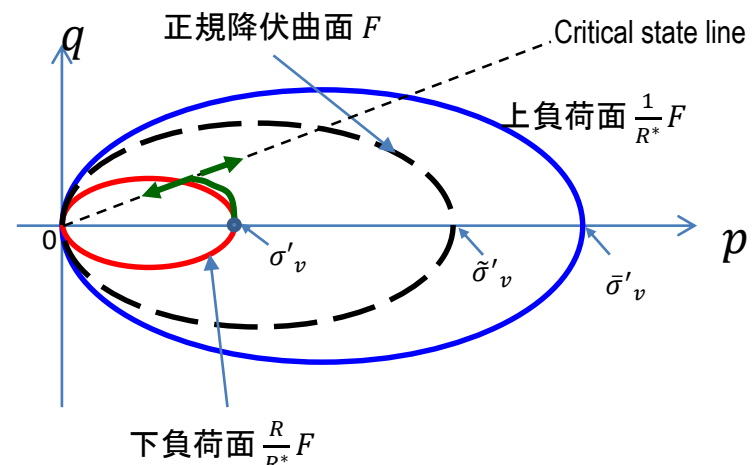
- Normal yield surface

$$F = MD \ln \left( \frac{p'}{p_0'} \right) + \frac{MD}{\eta_E} \left( \frac{\eta^*}{M} \right)^{\eta_E}$$

Where,  $M$  is critical state parameter,  $D$  is dilatancy factor,  $\eta_E$  is parameter controlling the shape of yield surface.

$$\eta^* = \sqrt{3/2} \left\| (1/p)\mathbf{s} - (1/p_0)\mathbf{s}_0 \right\|$$

Where,  $p$  and  $\mathbf{s}$  are the hydrostatic pressure and deviatoric stress tensor, respectively.



$$OCR = \frac{\bar{\sigma}'_v}{\sigma'_v}$$

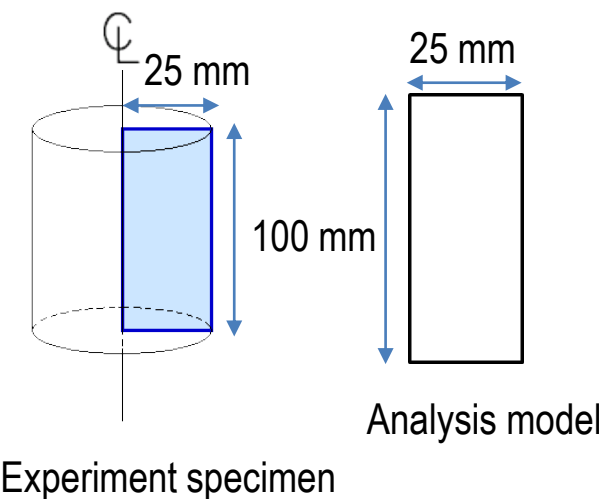
$$R = \frac{\sigma'_v}{\bar{\sigma}'_v}, R^* = \frac{\tilde{\sigma}'_v}{\bar{\sigma}'_v}$$

$$\frac{R^*}{R} = \frac{\frac{\tilde{\sigma}'_v}{\bar{\sigma}'_v}}{\frac{\sigma'_v}{\bar{\sigma}'_v}} = \frac{\tilde{\sigma}'_v}{\sigma'_v}$$

The sub-loading surface shall satisfy the following conditions

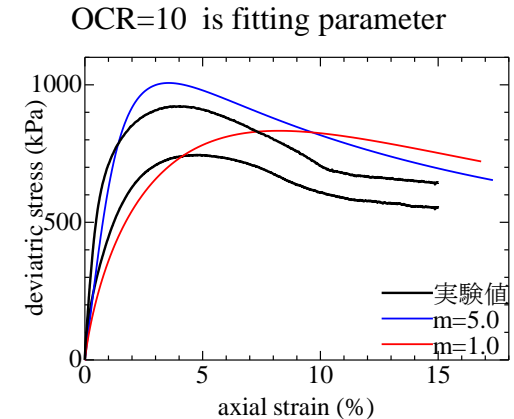
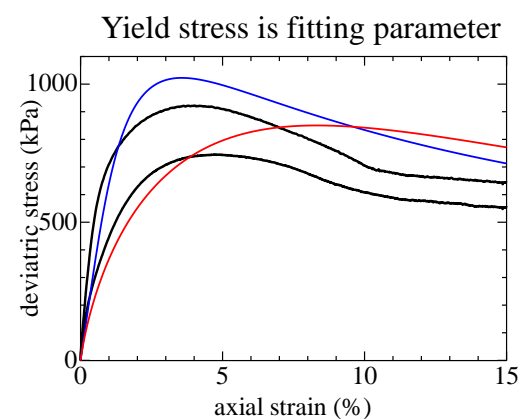
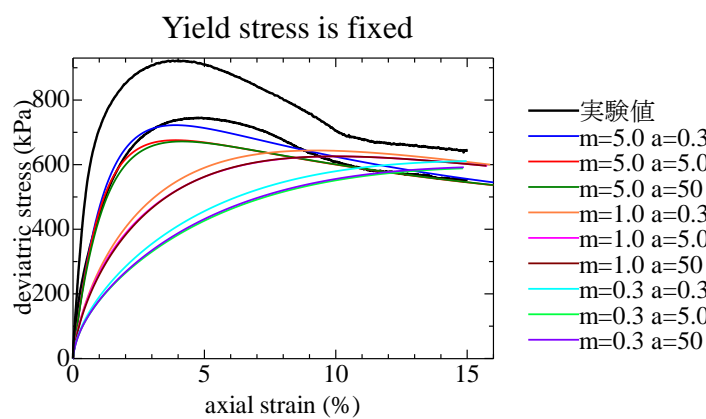
- Sub-loading surface is in similar shape as the normal yield surface.
- The current stress-point is always on sub-loading surface.
- Along with expansion of sub-loading surface, the normal yield surface also expands and thereby plastic deformation occurs.
- $R = 1$ : the sub-loading surface coincides with normal yield surface

# Parameter identification



テストNo.	$\rho(\text{g/cm}^3)$	w(%)	$e$	$S_r(%)$	$D_r(%)$	B値
002	1.99	23.22	0.64	96.15	53.45	0.84
003	1.94	16.89	0.60	74.59	67.88	0.86
004	1.96	16.92	0.58	77.28	74.99	0.82
005	1.95	16.75	0.59	74.89	70.46	0.84
006	1.95	16.44	0.59	74.61	73.71	0.82

テストNo.	試験装置	排水条件	拘束圧
002	スマート三軸試験	排水	157kPa
003	スマート三軸試験	排水	200kPa
004	従来の三軸試験	排水	50kPa
005	従来の三軸試験	排水	100kPa
006	従来の三軸試験	排水	200kPa



OCR=10, 拘束圧200kPa

# Material parameters

Elasto-plastic parameters		
S.No.	Parameter name	Value
1	Dilatancy ( $D$ )	0.065
2	Critical stress ratio ( $M$ )	1.41
3	Irreversible ratio $\Lambda$	0.973
4	Over-consolidation ratio ( $OCR$ )	10
5	Yield surface shape parameter $\eta_E$	1.5

Initial conditions		
S.No.	Parameter name	Value
1	Initial void ratio $e_0$	0.585
2	Swelling index $\kappa_0$	0.042
3	Coefficient of earth pressure $K_i$	1.0
4	Normal Yield stress $\tilde{\sigma}'_v$ (kPa)	180
5	Initial vertical stress $\sigma'_v$ (kPa)	20

Evolution parameter		
S.No.	Parameter name	Value
1	Sub-loading surface parameter ( $m_a$ )	5.0
2	Super-loading surface parameter ( $a = m_a/D$ )	76.92
3	Super-loading parameter ( $b, c$ )	1.0
4	Similarity ratio for sub-loading ( $R_0 = 1/OCR$ )	0.1
5	Similarity ratio for super-loading ( $R^*$ )	0.9

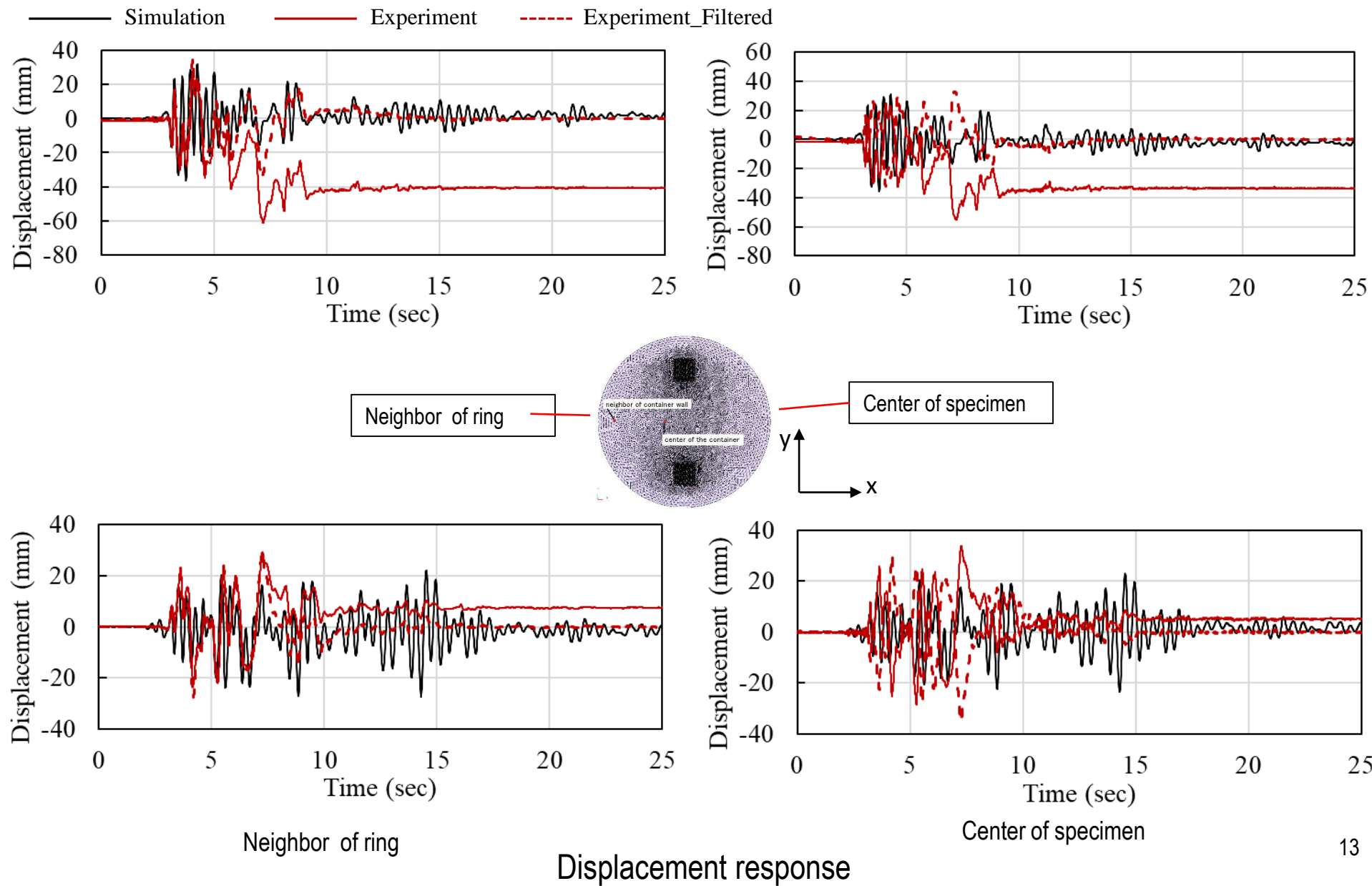
$$OCR = \frac{\bar{\sigma}'_v}{\sigma'_v}$$

$$R = \frac{\sigma'_v}{\bar{\sigma}'_v}, R^* = \frac{\tilde{\sigma}'_v}{\bar{\sigma}'_v}$$

$$\frac{R^*}{R} = \frac{\frac{\tilde{\sigma}'_v}{\bar{\sigma}'_v}}{\frac{\sigma'_v}{\bar{\sigma}'_v}} = \frac{\tilde{\sigma}'_v}{\sigma'_v}$$

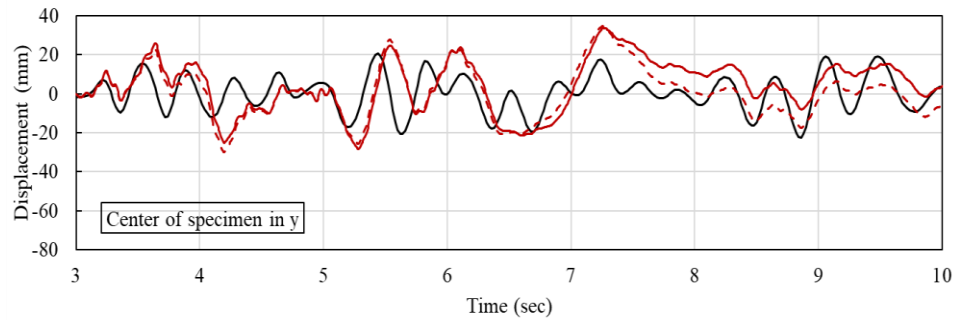
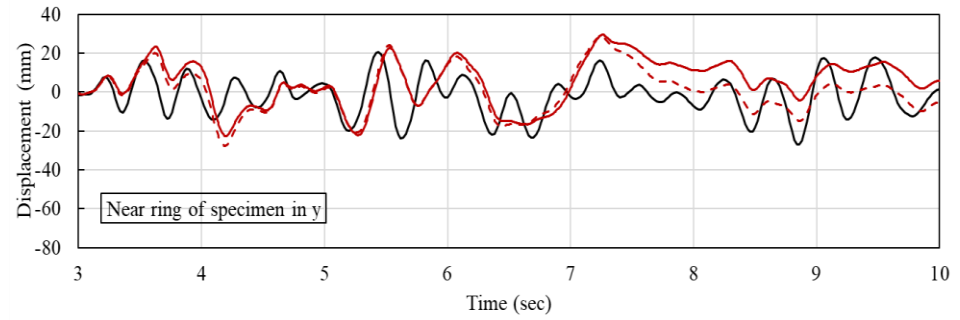
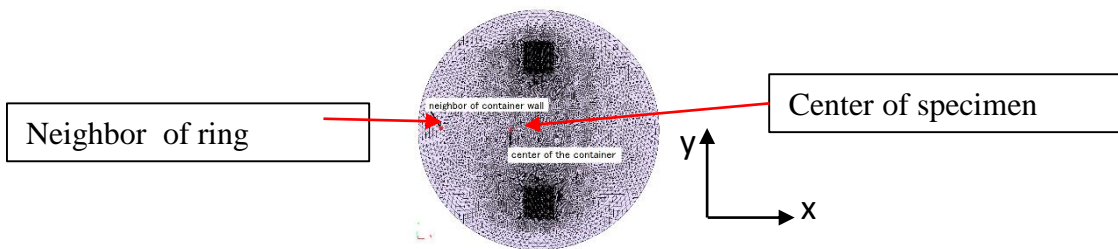
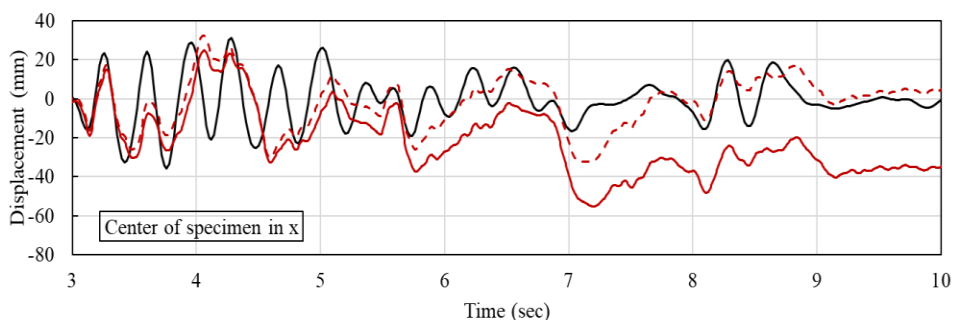
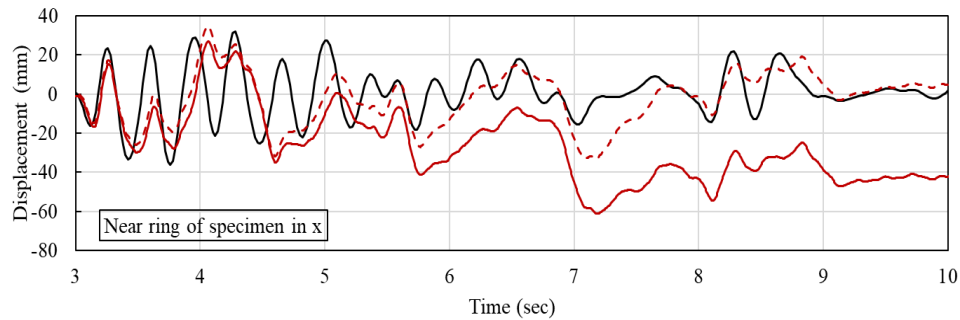
Here,  $\sigma'_v$ ,  $\tilde{\sigma}'_v$  and  $\bar{\sigma}'_v$  are the stress on sub-loading, normal yield surface, and super-loading surface.

# Displacement time history on top surface



# Displacement time history on top surface

— Simulation — Experiment - - - Experiment\_Filtered

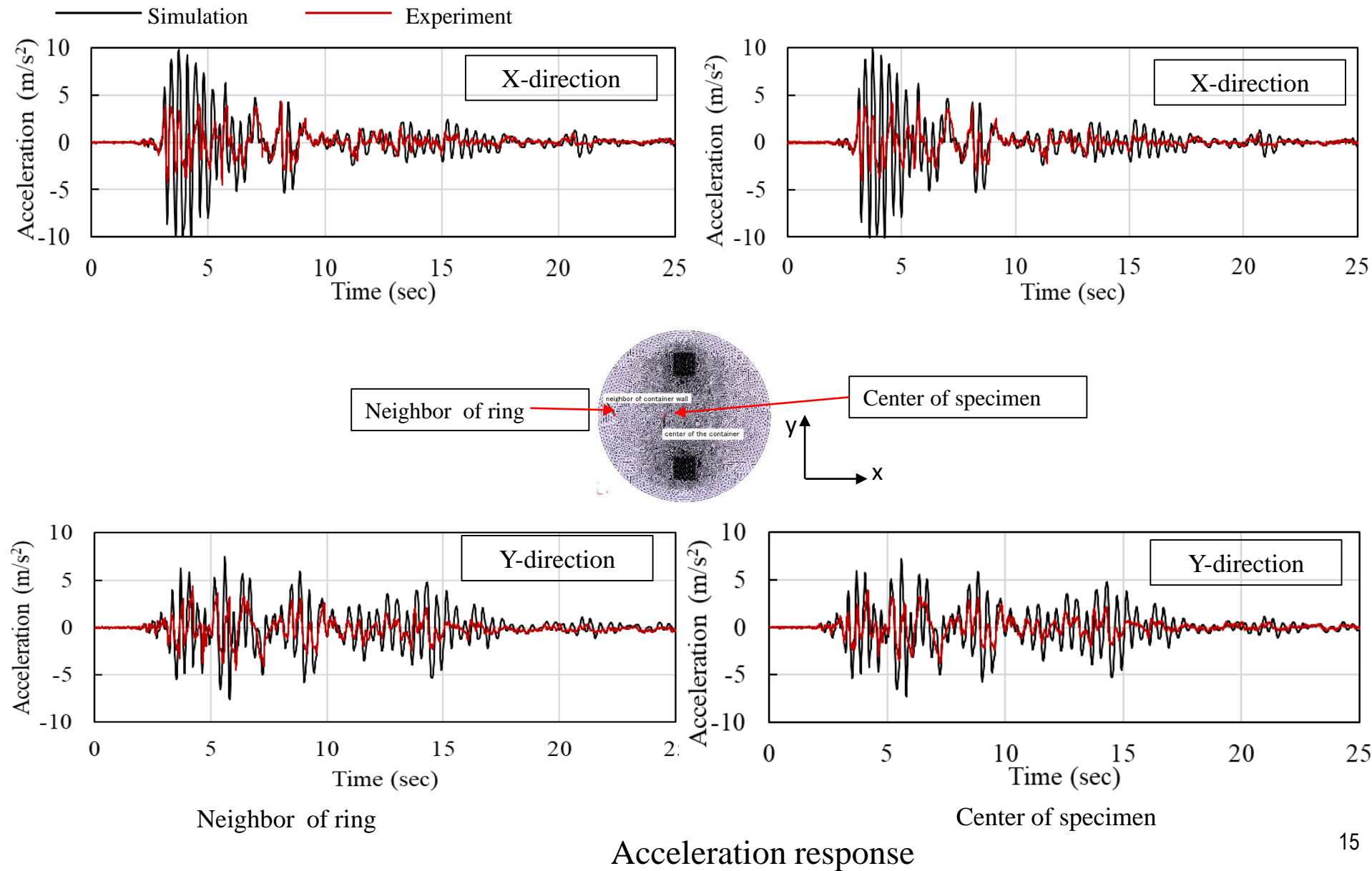


Neighbor of ring

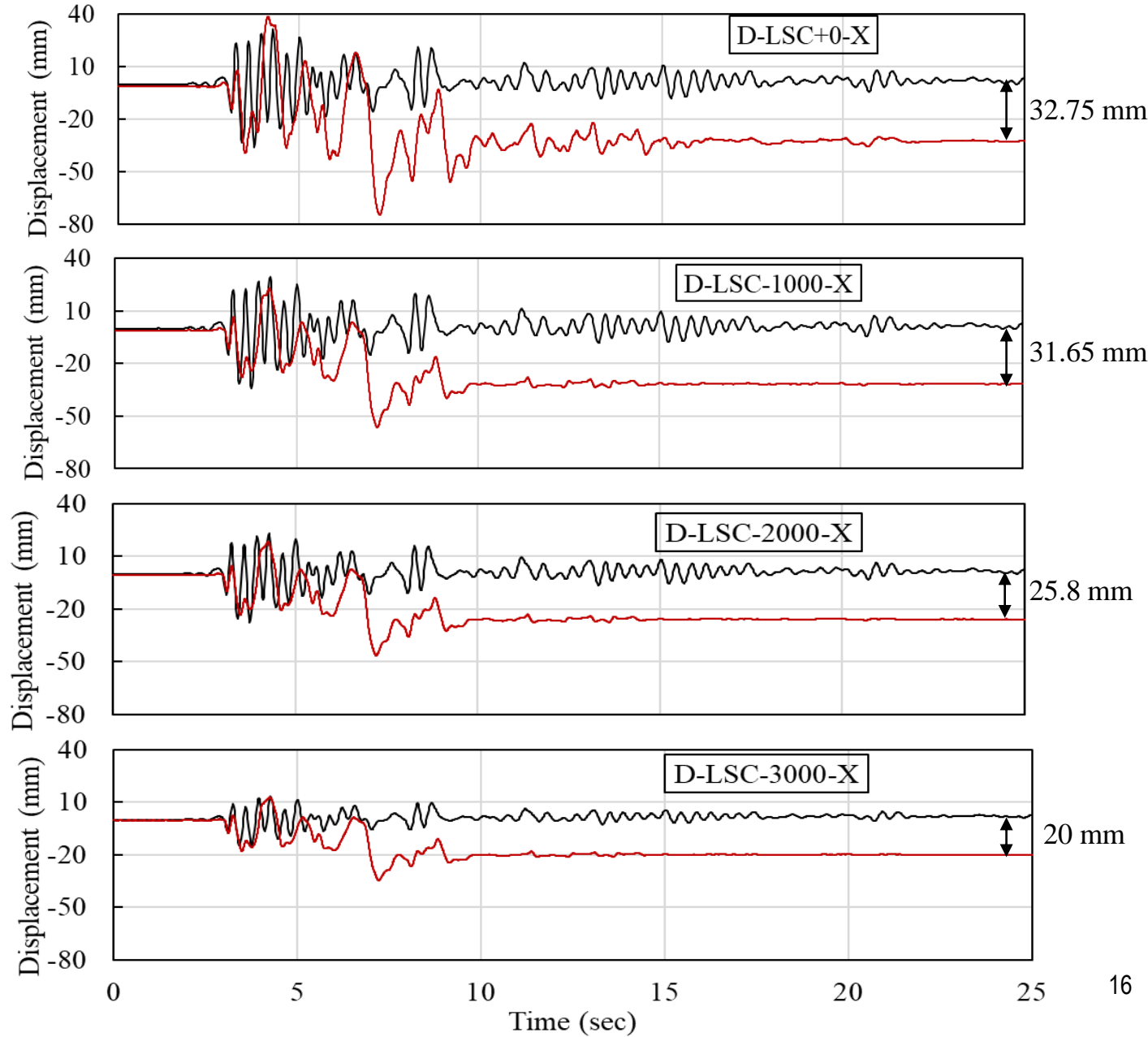
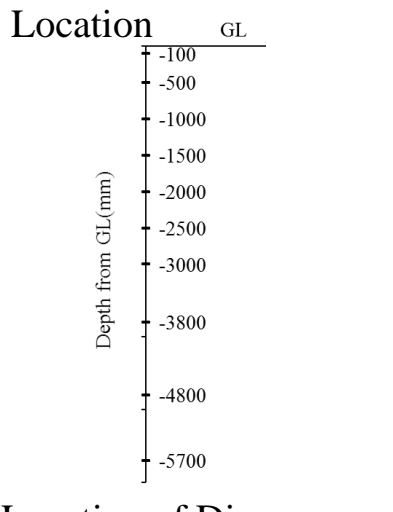
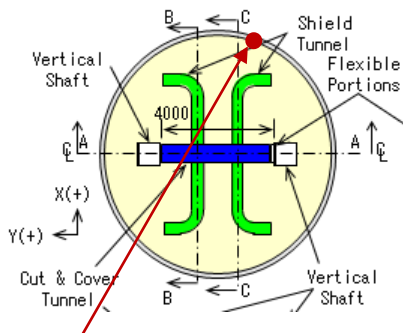
Displacement response

Center of specimen

# Acceleration time history on top surface



# Displacement time history



# Laminar soil container modeling

S. No	Items	Position	Weight (ton)	No of rings	Weight (ton)	Total	
1	Laminar rings	Top	3.1	1	3.1		
		Middle	0.9	19	17.1		
			1.0	19	19		
		Bottom	2.5	1	2.5	41.7	
2	Slider	SA			0.159		
		SB			0.058		
		SC			1.076	1.3	
3	Rubber	Water resistance			0.50		
		Slippage			0.25	0.75	
Total weight (1+2+3):						43.7	

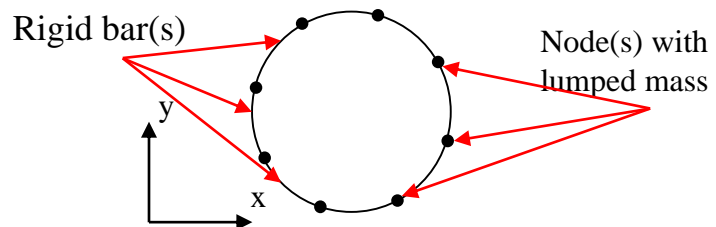
## Constrained condition (拘束条件)

$$\mathbf{r}_1^t - \mathbf{r}_0^t - \mathbf{R}(\theta_0^t) \cdot (\mathbf{r}_1^0 - \mathbf{r}_0^0) = 0$$

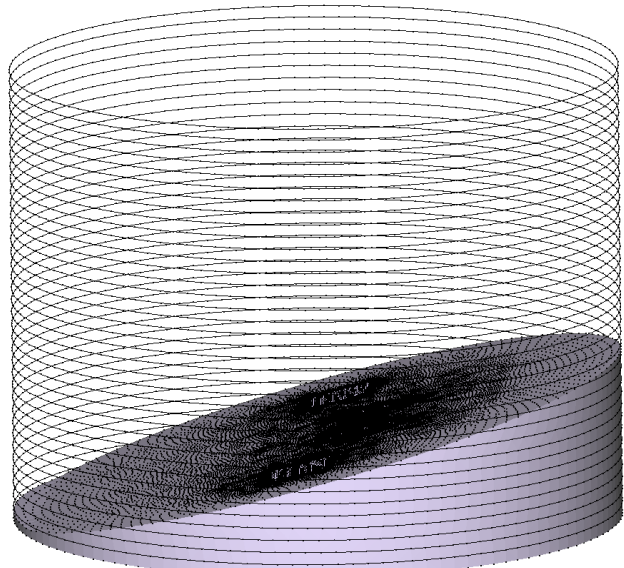
$$\theta_1^t - \theta_0^t = 0$$

Here,  $\mathbf{r}_i^t, \theta_i^t$  are position and rotation vector of  $i^{th}$  node at  $t^{th}$  time step, respectively.

$R(\theta)$  is rotation tensor corresponding to rotation vector  $\theta$



Graphical representation of laminar ring modeling

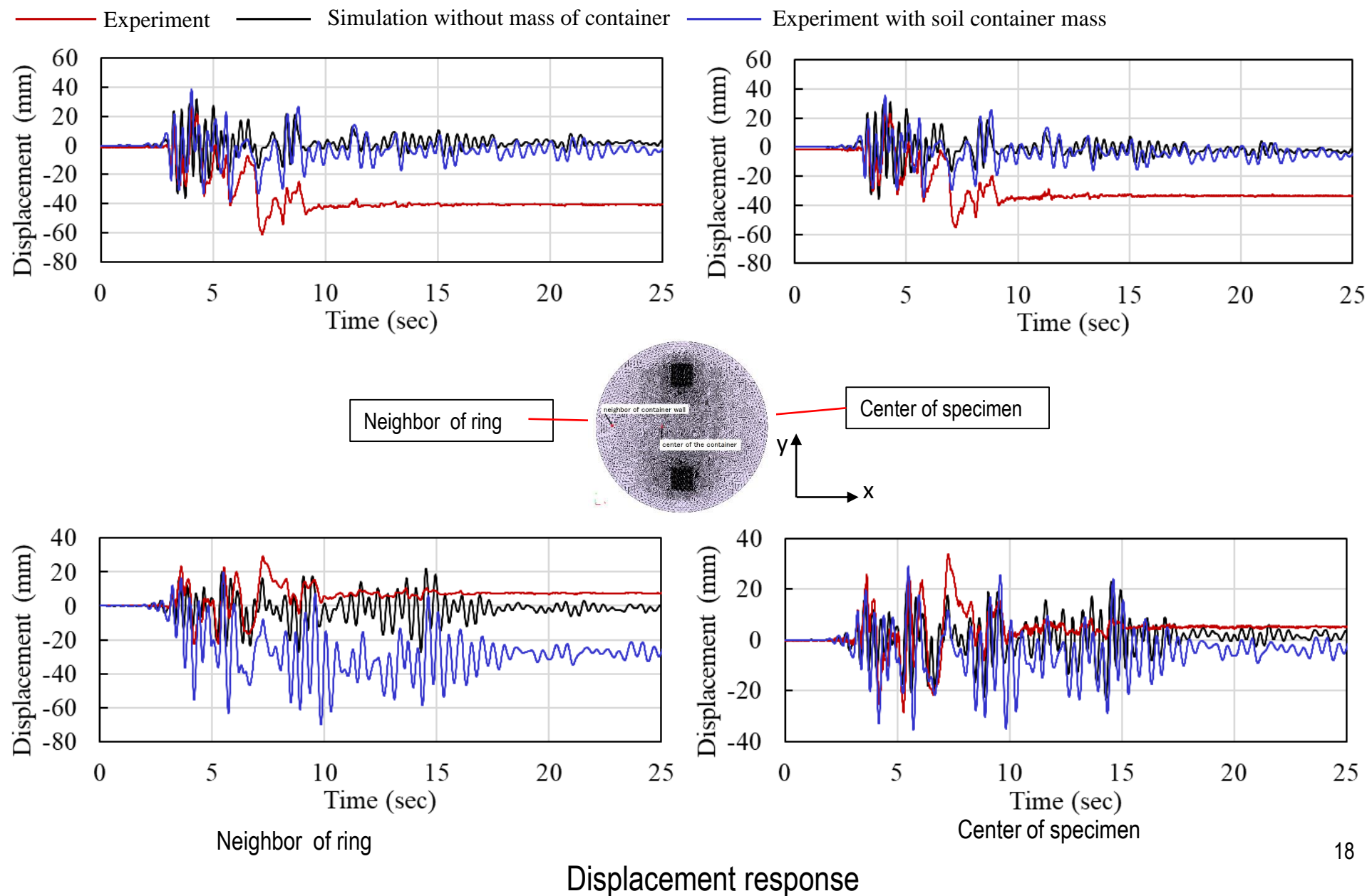


S. No	Position	Weight/ring (ton)	No of rings	Weight (ton)	Total (ton)
1	Top	3.1+0.055	1	3.155	
2	Middle	1.03+0.055	35	37.975	
3	Bottom	2.5+0.055	1	2.555	
					43.69

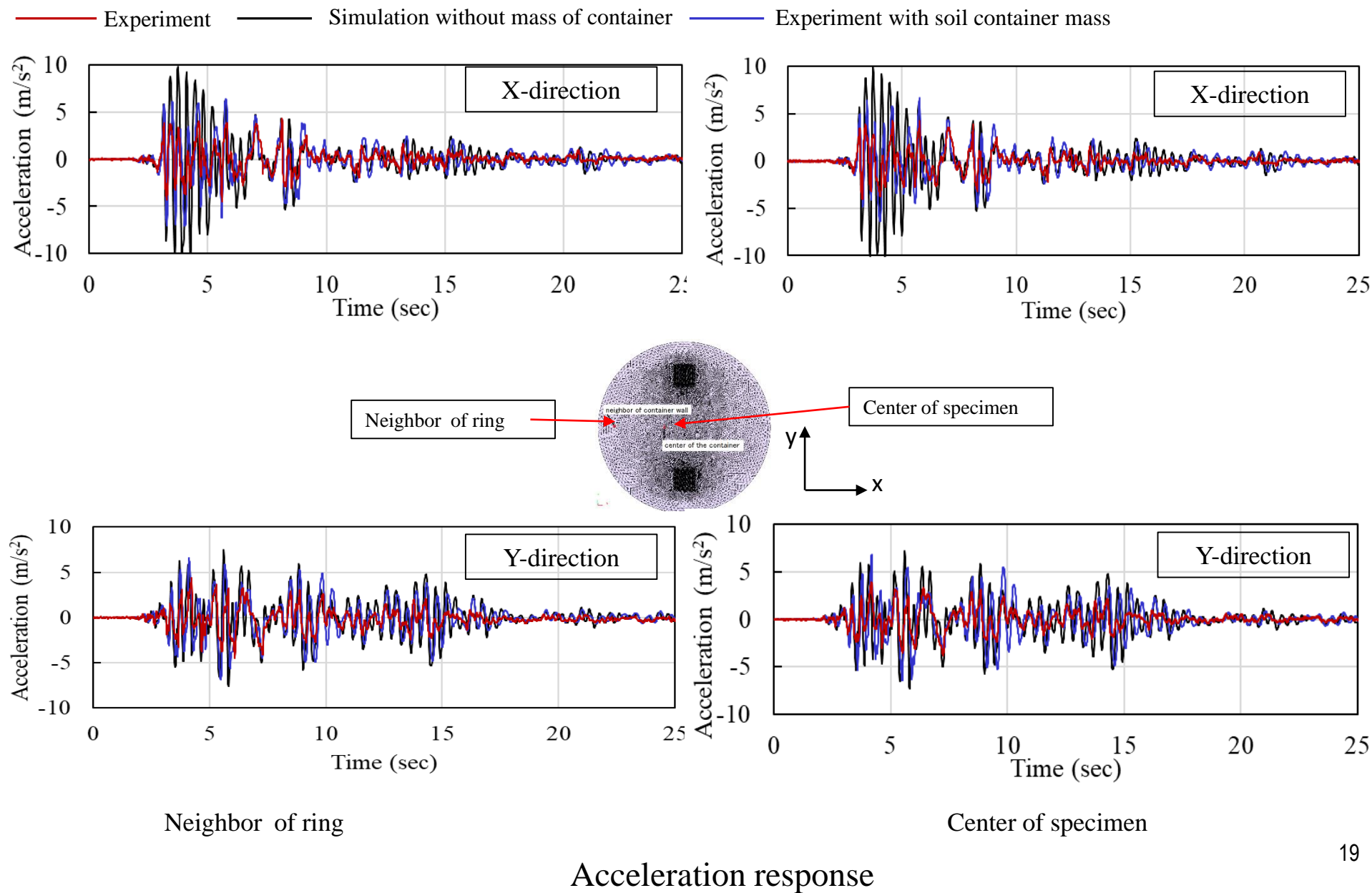
**Note:** Additional weight of rubbers and slider is equally distributed to all laminar rings. The value of contribution is equal to  $(2.05/37)=0.055$

Laminar rings with lumped mass at nodes

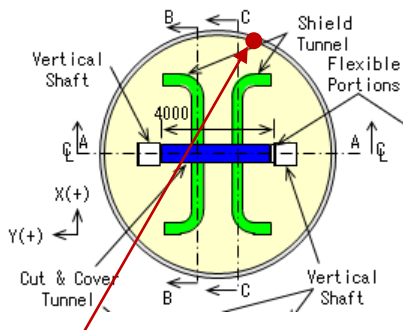
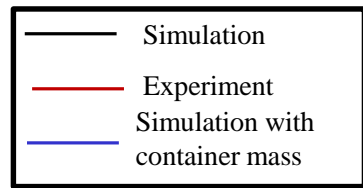
# Displacement time history on top surface



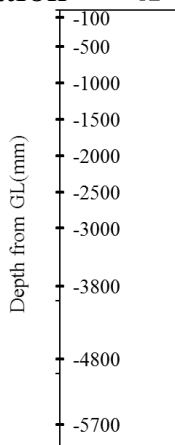
# Acceleration time history on top surface



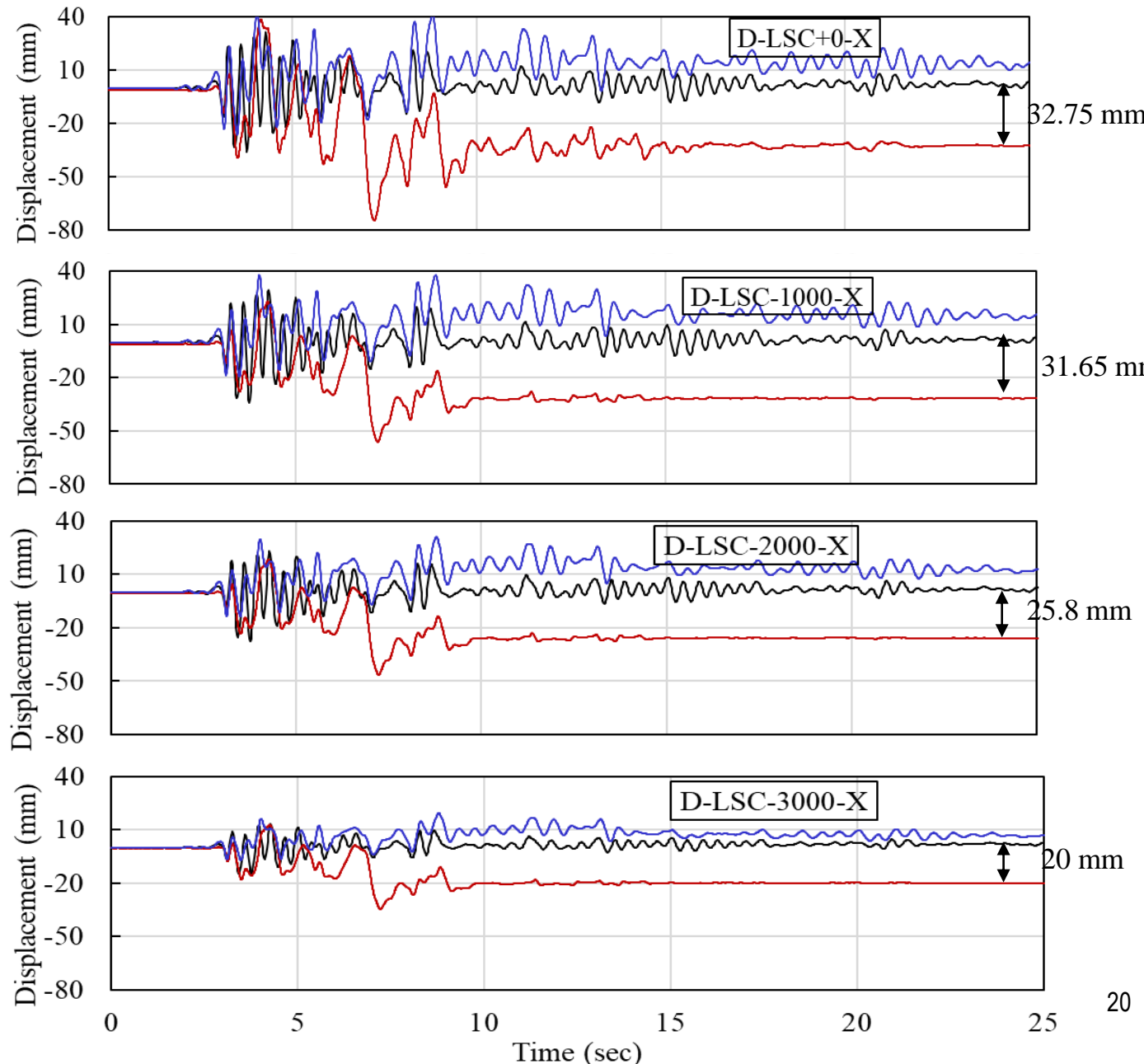
# Displacement time history



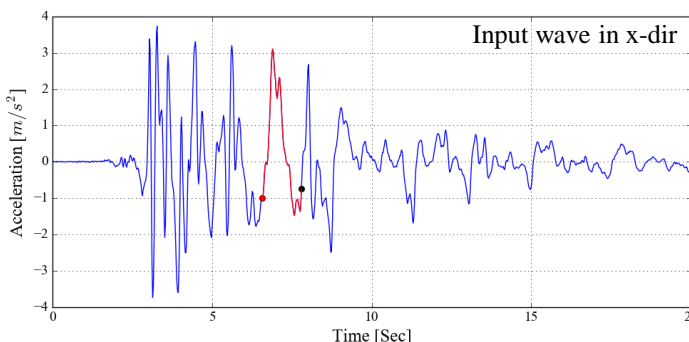
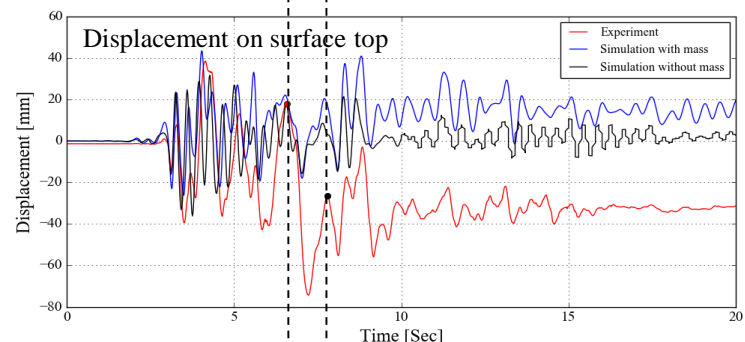
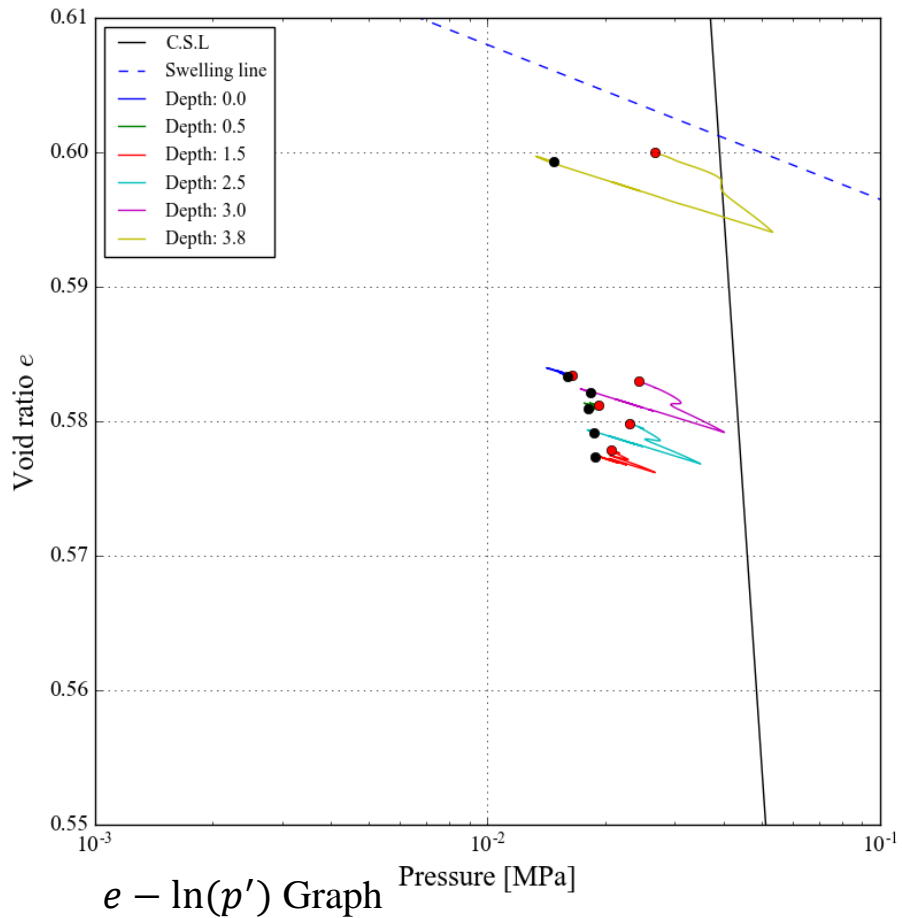
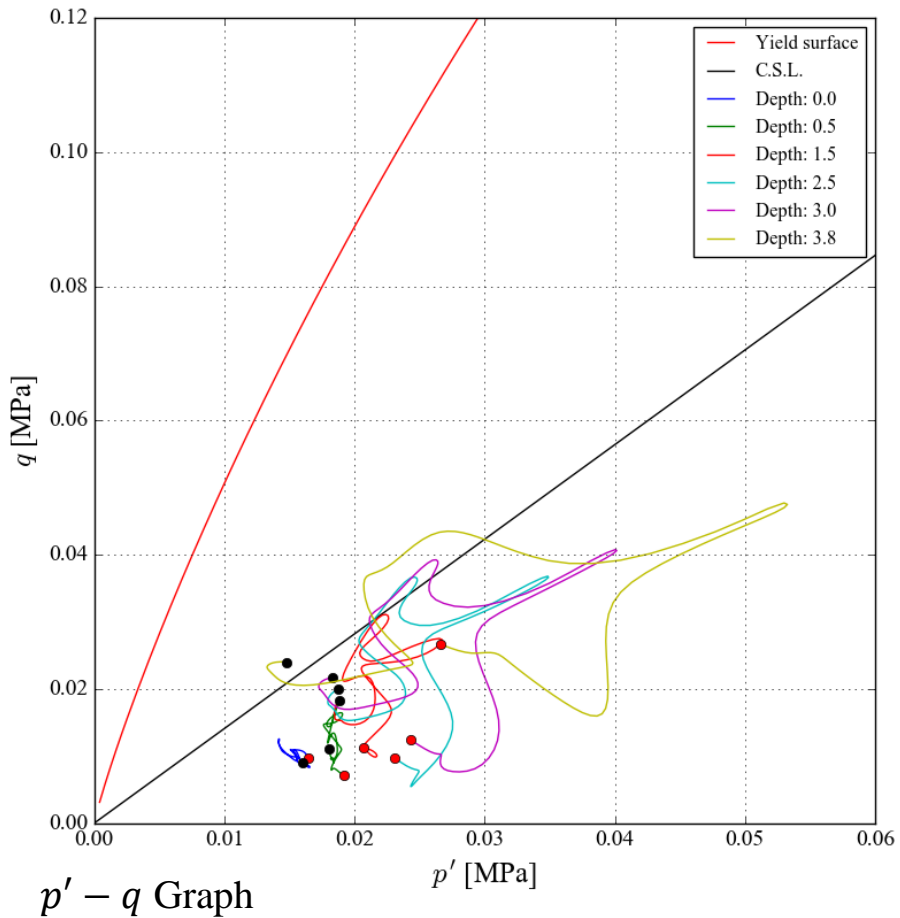
Location



Location of Disp. sensor



# Effective Stress path



# 今後の構想

# Summary and future work

- Acceleration time history results have good agreement with experimental results
- Except the residual deformation, displacement time history results also show reasonable agreement with experimental results.
- Incorporation of mass of laminar soil container may be essential to reproduce the residual deformation.
- Effective stress-path and  $e-\ln(p)$  graph suggest that
  - Soil in the vicinity of soil-strata interface is failing
  - Plasticity is inadequately modeled
- Re-simulation by lowering the value of OCR is planned for next work in the to-do list with an aim to increase the plasticity

Thank you for listening